

Arrival and diversification of mabuyine skinks (Squamata: Scincidae) in the Neotropics based on a fossil-calibrated timetree

Anieli Guirro Pereira ¹, Carlos G Schrago ^{Corresp. 1}

¹ Department of Genetics, Universidade Federal do Rio de Janeiro, Rio de Janeiro, RJ, Brazil

Corresponding Author: Carlos G Schrago
Email address: carlos.schrago@gmail.com

Background: The evolution of South American Mabuyinae skinks holds significant biogeographic interest because its sister lineage is distributed across the African continent and adjacent islands. Moreover, at least one insular species, *Trachylepis atlantica*, has independently reached the New World through transoceanic dispersal. To clarify the evolutionary history of both Neotropical lineages, this study aimed to infer an updated timescale using the largest species and gene sampling dataset ever assembled for this group. By extending the analysis to the Scincidae family, we could employ fossil information to estimate mabuyinae divergence times and carried out a formal statistical biogeography analysis. To unveil macroevolutionary patterns, we also inferred diversification rates for this lineage and evaluated whether the colonization of South American continent significantly altered the mode of Mabuyinae evolution.

Methods: A time-calibrated phylogeny was inferred under the Bayesian framework employing fossil information. This timetree was used to (i) evaluate the historical biogeography of mabuyines using the statistical approach implemented in BioGeoBEARS; (ii) estimate macroevolutionary diversification rates of the South American Mabuyinae lineages and the patterns of evolution of selected traits, namely, the mode of reproduction, body mass and snout-vent length; (iii) test the hypothesis of differential macroevolutionary patterns in South American lineages in BAMM and GeoSSE; and (iv) re-evaluate the ancestral state of the mode of reproduction of mabuyines.

Results: Our results corroborated the hypothesis that the occupation of the South American continent by Mabuyinae consisted of two independent dispersion events that occurred between the Oligocene and the Miocene. We found significant differences in speciation rates between the New World and the remaining Mabuyinae clades only in GeoSSE. The influence of phenotypic traits on diversification rates was not supported by any method. Ancestral state reconstruction suggested that the ancestor of South American mabuyine was likely viviparous.

Discussion: Our analyses further corroborated the existence of a transoceanic connection between Africa and South America in the Eocene/Oligocene period (Atlantogea). Following colonization of the isolated South America and subsequent dispersal through the continent by the ancestral mabuyine stock, we detected no difference in macroevolutionary regimes of New World clades. This finding argued against the ecological opportunity model as an explanation for the diversity of living mabuyines.

1 **Arrival and diversification of mabuyine skinks (Squamata: Scincidae) in the Neotropics**
2 **based on a fossil-calibrated timetree**

3

4 Anieli G. Pereira and Carlos G. Schrago*

5 *Department of Genetics, Federal University of Rio de Janeiro, RJ, Brazil*

6

7

8

9

10 *Corresponding author:

11 Instituto de Biologia, Departamento de Genética, CCS, A2-092

12 Rua Prof. Rodolpho Paulo Rocco, SN

13 Cidade Universitária

14 Rio de Janeiro, RJ

15 CEP: 21941-617

16 BRAZIL

17 Phone: +55 21 2562-6397

18 Phone: +55 21 4063-8278

19 Email: carlos.schrago@gmail.com

20 **Abstract**

21

22 **Background:** The evolution of South American Mabuyinae skinks holds significant
23 biogeographic interest because its sister lineage is distributed across the African continent and
24 adjacent islands. Moreover, at least one insular species, *Trachylepis atlantica*, has independently
25 reached the New World through transoceanic dispersal. To clarify the evolutionary history of
26 both Neotropical lineages, this study aimed to infer an updated timescale using the largest
27 species and gene sampling dataset ever assembled for this group. By extending the analysis to
28 the Scincidae family, we could employ fossil information to estimate mabuyinae divergence
29 times and carried out a formal statistical biogeography analysis. To unveil macroevolutionary
30 patterns, we also inferred diversification rates for this lineage and evaluated whether the
31 colonization of South American continent significantly altered the mode of Mabuyinae
32 evolution.

33 **Methods:** A time-calibrated phylogeny was inferred under the Bayesian framework employing
34 fossil information. This timetree was used to (i) evaluate the historical biogeography of
35 mabuyines using the statistical approach implemented in BioGeoBEARS; (ii) estimate
36 macroevolutionary diversification rates of the South American Mabuyinae lineages and the
37 patterns of evolution of selected traits, namely, the mode of reproduction, body mass and snout–
38 vent length; (iii) test the hypothesis of differential macroevolutionary patterns in South American
39 lineages in BAMM and GeoSSE; and (iv) re-evaluate the ancestral state of the mode of
40 reproduction of mabuyines.

41 **Results:** Our results corroborated the hypothesis that the occupation of the South American
42 continent by Mabuyinae consisted of two independent dispersion events that occurred between
43 the Oligocene and the Miocene. We found significant differences in speciation rates between the
44 New World and the remaining Mabuyinae clades only in GeoSSE. The influence of phenotypic
45 traits on diversification rates was not supported by any method. Ancestral state reconstruction
46 suggested that the ancestor of South American mabuyine was likely viviparous.

47 **Discussion:** Our analyses further corroborated the existence of a transoceanic connection
48 between Africa and South America in the Eocene/Oligocene period (Atlantogea). Following
49 colonization of the isolated South America and subsequent dispersal through the continent by the
50 ancestral mabuyine stock, we detected no difference in macroevolutionary regimes of New

51 World clades. This finding argued against the ecological opportunity model as an explanation for
52 the diversity of living mabuyines.

53 Introduction

54

55 The subfamily Mabuyinae comprises 24 genera and 197 species of lizards and belongs to
56 the highly diverse worldwide family, Scincidae (Lepidosauria; Squamata) (Uetz and Hosek,
57 2015). The Mabuyinae, as well as the Scincidae, are distributed on nearly all continents.
58 Approximately one-third of the species in this subfamily are from the Neotropical region, and
59 they are the only representatives of scincids in South America.

60 The entire diversity of mabuyine species was traditionally assigned to the single genus,
61 *Mabuya*, but a previous analysis proposed four new monophyletic genera with well-defined
62 geographical distributions (Mausfeld *et al.*, 2002): (1) *Trachylepis* (previously *Euprepis*),
63 comprising African and Madagascan species with one South American representative (*T.*
64 *atlantica*); (2) *Eutropis*, containing Asian species; (3) *Chioninia*, from the Cape Verde islands;
65 and (4) *Mabuya*, containing New World species, recently rearranged into 16 new genera by
66 Hedges and Conn (2012). Hedges and Conn (2012) treated South American Mabuyinae as a
67 clade of family Mabuyidae, within the superfamily Lygosomoidea. The new Mabuyidae
68 consisted of four new subfamilies: Mabuyinae, Chioniniinae, Dasiinae and Trachylepidinae.
69 Hedges and Conn's arrangement disregarded many genera previously related to Mabuyinae, such
70 as *Eutropis*, *Lankaskincus*, and *Ristella* (Pyron *et al.*, 2013), and recent papers have questioned
71 this classification (e.g. Pyron *et al.*, 2013, Pinto *et al.*, 2015, Karin *et al.*, 2016). Recently,
72 alternative classifications were suggested. For instance, Karin *et al.* (2016) placed the Middle-
73 Eastern *Trachylepis* (*T. aurata*, *T. vittatus*, and *T. septemtaeniatus*) into the genus *Heremites* and
74 *Eutropis novemcarinata* into *Toenayar novemcarinata*. Moreover, Pinto *et al.* (2015) assigned
75 species from the genera *Maracaiba* and *Alinea* back to genus *Mabuya* and Metallinou *et al.*

76 (2016) reclassified *Trachylepis ivensii* as *Lubuya ivensii*. In this study, we followed the Reptile
77 Database (Uetz and Hosek, 2015) taxonomy as of January 2017, which classified this clade as
78 subfamily Mabuyinae of the family Scincidae.

79 Therefore, at least two phylogenetically distinct lineages of Mabuyinae are distributed in
80 the New World, namely, *T. atlantica* and the Continental American Mabuyinae (CAM) clade.
81 These lineages are distinguished by both morphological features – presacral vertebrae counts,
82 keeled dorsal scales, coloration, and oviparity (Greer, 1970) – and molecular evidence (e.g.
83 Mausfeld and Vrcibradic, 2002; Carranza and Arnold, 2003; Whiting *et al.*, 2006). It is
84 customary to assume that the history of Mabuyinae in South American continent consisted of
85 two independent transoceanic dispersal events from the Old World (Mausfeld and Vrcibradic,
86 2002; Carranza and Arnold, 2003; Whiting *et al.*, 2006). The spatial distribution of the single
87 representative of the genus *Trachylepis* in an island closer to South America than to Africa, *T.*
88 *atlantica*, is of particular interest. This issue is so intriguing that it has reached the pages of
89 nontechnical literature (de Queiroz, 2014). *T. atlantica* is found in Fernando de Noronha, a small
90 volcanic archipelago in the Atlantic Ocean that lies 375 km from the northeastern coast of Brazil
91 and that was geologically formed from the Miocene (12.3 Ma) to the upper Pliocene, from 3.3 –
92 1.7 Ma (Almeida, 2002). Although other *Trachylepis* species have spread to several islands near
93 the African continent, the presence of *T. atlantica* in Fernando de Noronha likely represents the
94 farthest dispersal registered for the genus.

95 The CAM lineage, on the other hand, contains approximately 60 species of Mabuyinae.
96 Previous studies have suggested that the split between this clade and the African Mabuyinae
97 (genus *Trachylepis*) occurred from 28 – 34 Ma (Hedges and Conn, 2012; Karin *et al.*, 2016).
98 Additionally, the age of the last common ancestor (LCA) of the CAM was dated at 7 – 9 Ma

99 (Carranza and Arnold, 2003; Pinto-Sanchez et al., 2015) and 11 – 14 Ma (Miralles and Carranza,
100 2010; Hedges and Conn, 2012; Karin et al., 2016). Considering the present-day Atlantic Ocean
101 currents, Mausfeld *et al.* (2002) suggested that *T. atlantica* could have dispersed from the coast
102 of Southwest Africa to South America, but no work to date has comprehensively evaluated this
103 hypothesis. The older estimated ages could be consistent with the supposed faunal transoceanic
104 connection between Africa and South America during the Eocene/Oligocene (e.g. hystricognath
105 rodents, Loss-Oliveira *et al.*, 2012; Voloch *et al.*, 2013; anthropoid primates, Schrago *et al.*,
106 2012; 2013; amphisbaenians, Vidal *et al.*, 2008; emballonurid bats, Teeling, 2005; Leigh *et al.*,
107 2013; testudinid turtles, Le *et al.*, 2006) through a single or a series of islands constituting an
108 Atlantic Ocean Ridge (the Atlantogea paleo province) (Simpson, 1950; Poux *et al.*, 2006; de
109 Oliveira *et al.*, 2009; Ezcurra and Agnolin, 2012; de Queiroz, 2014). This transatlantic island
110 corridor, associated with a drop in the sea level in the Oligocene, could explain faunal exchanges
111 in this period (de Queiroz, 2014). Regarding *T. atlantica*, there is a lack of estimates of the age of
112 the separation between this species and its African sister lineage.

113 Chronological information is indispensable for a full understanding of the scenario
114 underlying the current geographic distribution and evolutionary history of extant lineages
115 (Sanmartín *et al.* 2008; Loss-Oliveira *et al.* 2012). However, estimates of divergence times
116 within the Mabuyinae have been hampered by the lack of fossils for Mabuyinae, which made
117 previous researchers rely on evolutionary rates borrowed from the literature (e.g., Carranza and
118 Arnold, 2003; Miralles and Carranza, 2010; Lima *et al.*, 2013; Barker et al., 2015; Karin *et al.*,
119 2016) or to employ biogeographic events as calibrations (Hedges and Conn, 2012; Pinto-Sanchez
120 et al., 2015) to derive the timescale of this lineage. The fossil record, however, has been
121 demonstrated to be much more informative than biogeographic events as a calibration tool

122 (Heads, 2011). The use of biogeographic events to time-calibrate phylogenies requires the
123 assumption of vicariant scenarios of diversification, which entails that the speciation is
124 synchronous with the breaking apart of landmasses, or that island colonization occurs
125 immediately following geological formation (Heads, 2011; Mello and Schrago, 2012).

126 Revealing the origin and diversification of the CAM clade and *T. atlantica* also requires a
127 robust phylogenetic hypothesis. Although it is generally accepted that *T. atlantica* is a member of
128 the genus *Trachylepis* and therefore excluded from the main diversification of the CAM, its
129 evolutionary affinity remains controversial (Mausfeld et al., 2002; Carranza and Arnold, 2003;
130 Whiting et al., 2006). Early proposed phylogenies of Mabuyinae used a maximum of 35 species,
131 a number that significantly underrepresents the diversity of this subfamily (Mausfeld et al., 2002;
132 Carranza and Arnold, 2003; Whiting et al., 2006). Hedges and Conn (2012) studied the CAM
133 clade exclusively and included 40 species, whereas the large-scale Squamata phylogeny of Pyron
134 et al. (2013), which contains 4,161 species, sampled 71 mabuyine skink species. Recently, Pinto
135 Sanchez et al. (2015) used 250 specimens to infer the phylogeny and species diversity of
136 neotropical mabuyinaes, focusing on Colombian populations. Karin et al. (2016) analyzed the
137 higher-order relationships of Mabuyinae using 22 species (24 specimens). Considering that
138 improvements in phylogenetic inference and divergence time estimation can be obtained by
139 increasing taxon sampling (Linder et al., 2005; Albert et al., 2009; Soares and Schrago, 2012),
140 this matter requires further investigation.

141 Moreover, the occupation of the South American mainland by the CAM motivates an
142 analysis of differential rates of diversification and rates of phenotypic traits evolution in this
143 clade. It has been broadly reported that the ecological opportunity of a new environment can
144 induce acceleration of macroevolutionary rates (Yoder et al., 2010; Liedtke et al., 2016). This

145 phenomenon was documented for insular vertebrates (Losos JB, Mahler DL. 2010; Jonsson KA
146 et al. 2012); but, as proposed by G.G. Simpson (1953), the occupation of a new continent also
147 could trigger evolutionary radiations (Yoder JB et al. 2010; Pires MM, Silvestro D, Quental TB.
148 2015).

149 In this study, as a means of exploring the continental biogeographic and evolutionary
150 patterns associated with the occupation of South America by mabuyine skinks, we estimated the
151 molecular phylogeny and inferred the divergence times of its members employing fossil
152 information. The inferred time-tree was used to perform, for the first time, a formal statistical
153 analysis of the historical biogeography and macroevolutionary diversification rates of
154 Mabuyinae. To this end, by combining previously published data, we assembled the largest
155 dataset of species and gene sampling composed to date, with the aim of uncovering the evolution
156 of the Mabuyinae.

158 **Materials and Methods**

159

160 *Data collection, alignment, and taxonomy*

161 We assembled a chimeric supermatrix from previously published sequence data available
162 in GenBank. A total of eight genetic loci from 117 species of Mabuyinae, as well as 103
163 additional Scincid genera were analyzed, summing 220 taxa, with two genera of the family
164 Xantusiidae used as outgroups. All seven genes available from *Trachylepis atlantica* were used
165 in our analysis: the mitochondrial ribosomal genes *12S rRNA*, *16S rRNA* and the coding gene
166 *cytochrome b (cytb)*; as well as the nuclear genes alpha enolase (*enol*), oocyte maturation factor
167 (*cmos*), glyceraldehyde-3-phosphate dehydrogenase (*gapdh*), myosin heavy chain (*myh*), and G
168 protein-coupled receptor 149 (*gpr149*). The accession numbers are available in Supplementary
169 File 1. When several sequences representative of each taxon were available, the longest sequence
170 was selected. In order to simultaneously decrease the number of missing data and to increase the
171 number of representative taxa, we assumed genera and species as monophyletic. Therefore,
172 chimeric supermatrices were used. All protein-coding sequences were visually checked for stop
173 codons and aligned individually in SeaView v. 4.4.3 (Gouy *et al.*, 2010) using the MUSCLE v.
174 3.8.31 (Edgar 2004) algorithm, whereas the ribosomal genes were aligned in MAFFT v. 7 (Kato
175 and Standley, 2013). Gblocks v. 0.91b (Castresana, 2000; Talavera and Castresana, 2007) was
176 used to exclude poorly aligned bases and divergent regions in the *12S rRNA*, *16S rRNA*, and *enol*
177 genes. Individual genes were then concatenated into a single supermatrix using the R package
178 Phyloch (Heibl, 2015). RogueNarok (Aberer *et al.*, 2013) was used to identify taxa without
179 significant phylogenetic information using a ML tree and associated bootstrapped topologies.
180 These datasets were inferred under a rapid bootstrapping algorithm analysis with 200 replicates

181 (Stamatakis et al., 2008), followed by a thorough search of the ML tree using the evolutionary
182 model GTRGAMMA, performed in RAxML-HPC (8.1.24) (Stamatakis, 2014). Based on the
183 relative bipartition information criterion (RBIC) inferred by RogueNarok, the terminal nodes
184 *Larutia* and *Otosaurus* (RBIC > 1.0), were removed from the analysis. Another dataset,
185 assembled with a more stringent (RBIC > 0.5) criterion, was composed for comparison. Under
186 this criterion, the genus *Lankascincus* and the mabuyine species *Eumecia anchietae* and
187 *Trachylepis acutilabris* were excluded from the analyses. The results, however, were robust for
188 both RBIC values, and we report the results under RBIC > 1.0 hereafter. The final supermatrix
189 consisting of 4,131 base pairs are available in Supplementary File 2, and detailed information on
190 each locus of the final alignment was listed in Table 1.

191

192 *Evolutionary analyses*

193 We investigated 18 candidate partitioning schemes using PartitionFinder heuristic search
194 algorithm with the Bayesian information criterion (BIC) for model selection (Lanfear *et al.*,
195 2012). The partitioning schemes also tested codon positions of protein-coding genes. The
196 partitioning strategy with the best fit consisted of 7 partitions (Supplementary File 3), which
197 were used throughout the analyses. Maximum likelihood (ML) phylogenetic inference was
198 performed in RAxML-HPC (8.1.24) employing the evolutionary model GTRCAT. The GTR
199 substitution model was applied to each partition, as this is the only model supported in RAxML.
200 ML analyses used 200 initial searches for finding the optimal tree topology. Statistical support
201 for clades was assessed using 2,000 standard nonparametric bootstrap replicates (PB).

202 Inference of node ages was performed with the mcmctree program of the PAML 4.8a
203 package (Yang, 2007). For large alignments, the Bayesian inference of node ages via Markov

204 chain Monte Carlo is computationally intensive. To make the analyses feasible, we used an
205 approximate likelihood calculation modified from Thorne et al. (1998) and implemented in
206 memctree (Reis and Yang, 2011). Priors for the ρ gene and σ^2 parameters were set as $G(2,$
207 $200)$ and $G(1, 10)$, respectively. Markov chains were sampled every 1,000 generations until
208 50,000 trees were collected. The analysis was performed twice to check for convergence of the
209 chains. Effective sample sizes (ESS) of parameters were calculated in Tracer v. 1.5, and all
210 values were greater than 200.

211

212 *Calibration priors*

213 The age of the root, which corresponds to the split between the families Scincidae and
214 Xantusiidae, was calibrated at a minimum value of 70.6 Ma and a maximum age of 209.5 Ma.
215 The minimum was set according to the oldest scincid from the Late Cretaceous of North
216 America (Campanian, 83.5 – 70.6 Ma), as previously adopted by Mulcahy *et al.* (2012) (Rowe *et*
217 *al.*, 1992); while the maximum was set according to Benton *et al.* (2015), which proposed a
218 maximum age of the ancestral of Squamata. Additional calibration information was gathered
219 from the Paleobiology Database (paleobiodb.org) and entered as minimum ages of the stem nodes of
220 clades. The minimum age of the Scincidae stem node was calibrated at 20.4 Ma, based on the
221 oldest crown scincid *Eumeces antiquus* classified as a member of the subfamily Scincinae
222 (Holman, 1981; Estes, 1983). The stem node of the clade containing the extant genus *Eumeces*
223 was calibrated at a minimum age of 13.6 Ma based on fossils from the Middle Miocene in North
224 America (Holman, 1966; Voorhies *et al.*, 1987; Joeckel, 1988). The age of an extinct *Egernia* sp.
225 from the Miocene of Hungary (>5 Ma) was used to calibrate the stem node of the clade
226 containing this extant genus (Venczel and Hír, 2013). According to Böhme (2010), the fossil

227 *Tropidophorus bavaricus* belongs to extant genus *Tropidophorus*, and it was used to calibrate the
228 stem node of this clade, setting its minimum age at 13.6 Ma (Böttcher *et al.*, 2009). Calibration
229 nodes are shown in the Supplementary Figure 4.

230

231 *Ancestral area reconstruction*

232 A historical biogeographical reconstruction was performed for the subfamily Mabuyinae and its
233 sister clade (*Lankascincus* and *Ristella*). The R package BioGeoBEARS (Matzke 2013) was used
234 to run likelihood methods: DIVALIKE (a likelihood interpretation of DIVA that allows for the
235 same events as DIVA – Matzke, 2013) and DEC (Dispersal-Extinction-Cladogenesis, Ree and
236 Smith, 2008). In BioGeoBEARS, we used the likelihood ratio to test whether the null models
237 (DIVALIKE and DEC) fitted the data better than did the more sophisticated models
238 (DIVALIKE+J and DEC+J). The “J” in models represents the addition of the founder-event
239 speciation, thereby allowing dispersal without range expansion (Matzke 2014). The maximum
240 range size, which limits the number of areas defined by tips and nodes, was set to two, based on
241 the current geographic distribution of species. Constraints on dispersal or area availability were
242 not included. To make the biogeographic analysis computationally feasible, islands were not
243 considered independent regions. The rationale for choosing the seven biogeographic areas
244 follows the zoogeographical regions found in the herpetological and biogeographical literature
245 (Vitt and Caldwell, 2009; Lomolino, 2010; Morrone, 2014; Pyron, 2014): (1) Neotropical
246 Brazilian Subregion (B), (2) Neotropical Chacoan Subregion (C), (3) West Indies – Caribbean
247 Islands (W); (4) Oriental Region (O): Southeast Asia + Philippines + Indian Subcontinent
248 (Pakistan to Bangladesh, including Sri Lanka, Nepal, and Bhutan); (5) Afrotropical (A): Sub-
249 Saharan Africa; (6) Madagascar (M): Madagascar and adjacent islands (the Seychelles and the

250 Comoros); and (7) Saharo-Arabian (S): Europe + North Africa + the northern portion of the
251 Arabian Peninsula + Southwest Asia. Using online distributional data from the Reptile Database
252 (Uetz and Hosek, 2015), we classified the tips as belonging to one or more of these areas.

253

254 *Rate of species diversification and diversification-phenotype rate correlation*

255 Our dated phylogeny of Mabuyinae was used to infer the dynamics of species
256 diversification using BAMM 2.5 (Bayesian Analysis of Macroevolutionary Mixtures – Rabosky,
257 2014), which simultaneously accounts for variation in evolutionary rates through time and
258 among lineages using transdimensional (reversible-jump) Markov chain Monte Carlo (rjMCMC)
259 (Rabosky 2014). Markov chains were sampled every 1,000th generation until 37,500 trees were
260 collected after a burn-in of 25%. Prior distributions were set according to *setBAMMPriors*
261 function from the BAMMtools R package (Rabosky *et al.* 2014). The frequencies of the species
262 in each genus were considered.

263 We also tested for trait-dependent diversification. The following traits were collated from the
264 literature: (i) data on the reproductive mode for 60 species of the Mabuyinae – 39 species as
265 viviparous, 17 as oviparous, and 3 as ovoviviparous (Meiri *et al.* 2013; Pyron and Burbrink
266 2013); (ii) the SVL (snout–vent length) for 46 species (Meiri 2010; Miralles and Carranza, 2010;
267 Das 2010; Hedges and Conn, 2012; Meiri *et al.* 2013; Pyron and Burbrink 2013); and (iii) the
268 body mass data for 35 species (Meiri 2010; Hedges and Conn, 2012). Following previous works,
269 we treated "ovoviviparity" as viviparity (Pyron and Burbrink 2013).

270 Differences in the rates of speciation (λ) and extinction (μ) between New World (*NW*)
271 and Old World (\overline{NW}) areas and between viviparous (*V*) and non-viviparous (\overline{V}) lineages were
272 tested using two approaches. Firstly, an ANOVA, implemented in the R package *diversitree*

273 (FitzJohn 2012), was used to compare different macroevolutionary regimes. In the NW/\overline{NW}
274 comparison, rates were calculated using the GeoSSE approach (Goldberg *et al.* 2011), whereas
275 BiSSE was used to test V/\overline{V} rates, with both tests of binary characters as implemented in
276 diversitree. In this sense, GeoSSE first optimised the parameters under an unconstrained full
277 model, in which ML estimates were obtained for (i) the speciation rate of the New World lineage
278 (λ_{NW}); (ii) the speciation rate of non-New World lineages ($\lambda_{\overline{NW}}$); (iii) the extinction rate of the
279 New World clade (μ_{NW}); (iv) the extinction rate of non-New World lineages ($\mu_{\overline{NW}}$); (v) the
280 intermediate speciation rate parameter ($\lambda_{NW,\overline{NW}}$); (vi) the dispersal rates from the New World
281 clade ($d_{NW\rightarrow\overline{NW}}$); and (vii) the dispersal rates of the sister lineages ($d_{\overline{NW}\rightarrow NW}$). Similarly, BiSSE
282 was used to infer (i) the speciation rate of the viviparous lineage (λ_V); (ii) the speciation rate of
283 non-viviparous lineages ($\lambda_{\overline{V}}$); (iii) the extinction rate of the viviparous clade (μ_V); (iv) the
284 extinction rate of non-viviparous lineages ($\mu_{\overline{V}}$); (v) transition rates from the viviparous clade (
285 $q_{V\rightarrow\overline{V}}$); and (vi) transition rates of the sister clade ($q_{\overline{V}\rightarrow V}$). Initial parametric values were set
286 according to the *starting.point* function from the diversitree package with an initial ratio of 0.5.
287 This preliminary step was required to build the likelihood function (the *make* command). In
288 BiSSE, species with unknown states were coded as ‘NA’ and assigned the sampling fraction of
289 the species of Mabuyinae used in this work (~61%), independent of the character state.
290 Subsequently, to perform the ANOVA test of the GeoSSE results, we chose to constrain the
291 intermediate speciation and the dispersal rate parameters to zero ($\lambda_{NW,\overline{NW}} = d_{NW\rightarrow\overline{NW}} =$
292 $d_{\overline{NW}\rightarrow NW} = 0$), in order to compare speciation and the extinction rates within regions exclusively.
293 Finally, we tested macroevolutionary alternative models against the full models (Table 2).

294 The second comparison between NW/\overline{NW} and V/\overline{V} macroevolutionary regimes used the

295 marginal posterior distributions of macroevolutionary parameters, inspected using the R package
296 diversitree. These distributions were obtained using the MCMC analyses, with samples taken in
297 diversitree every 1,000th generation until 1,000 samples were collected. A broad exponential
298 prior (mean of 0.5) for all parameters was used, as recommended, while the λ and μ rates were
299 set as the values obtained in the ML full model (FitzJohn 2012). For the NW/\overline{NW} relationship,
300 we also used the marginal posterior distributions obtained from BAMM, applying the
301 *getCladeRates* function of the BAMMtools R package. For all approaches, we calculated the
302 95% highest posterior density (HPD) interval for the difference between the means of the $NW/$
303 \overline{NW} and V/\overline{V} lineages (Bolstad 2007).

304 The diversification-phenotype rate correlation was performed in STRAPP (Rabosky and
305 Huang 2015), as implemented in BAMMtools. To run STRAPP, phylogenies were pruned to
306 match the available information for both tree terminals and traits. Diversification analysis results
307 previously obtained using BAMM were pruned to match the available trait information using the
308 function *subtreeBAMM* and were tested against the analyzed traits, using the Mann-Whitney
309 method for binary characters and both Pearson and Spearman methods for continuous traits.

310

311 *Rate of trait evolution and ancestral state reconstruction*

312 We inferred ancestral states of reproductive mode in the BayesTraits software (Pagel *et*
313 *al.* 2004) and in the R package BiSSE. Both approaches use the maximum likelihood method and
314 allow the use of species with unknown character states. Results were visualized in the R package
315 diversitree. The rates of trait evolution of the two continuous traits studied, namely, SVL and
316 body mass, were inferred in BAMM, using logarithms of both measures. Phylogenies were also
317 pruned to match the available information for both tree terminals and traits. We tested the

318 correlation between SVL and body mass using phylogenetic independent contrasts (PIC;
319 Felsenstein, 1985) as implemented in the R package *ape*. Prior distributions to these subtrees
320 were set according to *setBAMMPriors* function from the *BAMMtools* R package (Rabosky *et al.*
321 2014). Chains were sampled every 1,000 generations until 50,000 trees were collected. The
322 results were summarized and visualized in *BAMMtools*.

323 **Results**

324

325 Mabuyinae was recovered as a monophyletic group (BS = 76). The first split in this
326 subfamily isolated the genus *Dasia* from the remaining Mabuyinae and was inferred to have
327 occurred at 30 Ma, with an HPD interval ranging from 20 – 48 Ma (Supplementary File 4). The
328 biogeographical model with the highest likelihood was the DEC+J (lnL: -94.34). Therefore, the
329 addition of the J parameter for founder events significantly increased the likelihood of the DEC
330 model ($p = 1.2e^{-9}$, Table 3). Our results supported a model in which the genera *Lankascincus* and
331 *Ristella* split from Mabuyinae (BS = 20) in the Oriental region.

332 After dispersal from the Oriental region to Africa, the ancestor of the CAM clade split
333 from Saharo-Arabian *Trachylepis* approximately 25 Ma ($\pm 16 - 41$ Ma) (BS=60). Subsequently,
334 the stock that gave rise to New World Mabuyinae dispersed from the Saharo-Arabian region to
335 the Neotropical Brazilian Subregion (Figure 1). The New World Mabuyinae were recovered as
336 monophyletic (BS=97), and the age of their LCA was estimated as 19 Ma (12 – 31 Ma). Our
337 results supported the hypothesis that this lineage reached the Neotropics via the Brazilian
338 Subregion. From this region, the ancestor of *Spondylurus* and *Copeoglossum* dispersed to islands
339 of the West Indies. The continental clade later dispersed along the Brazilian Subregion.
340 Additional dispersal events to the West Indies were inferred to have occurred at least twice: in
341 the ancestor of *Mabuya* and in that of *Alinea* and *Marisora*. *Marisora* was not recovered as
342 monophyletic, with the Central American clade as sister to *Alinea* and the South American clade
343 as sister to *Aspronema*.

344 The origin of *Trachylepis atlantica* consisted of a different history. Firstly, the
345 monophyly of genus *Trachylepis* was not recovered. This genus was split into two lineages: one

346 sister lineage of the CAM clade and another major clade to which *T. atlantica* belongs. Our
347 analysis supported the phylogenetic position of *T. atlantica* as a sister lineage of the clade
348 including the Europa Island *T. infralineata*, the Madagascan *T. comorensis*, and the continental
349 African *T. maculilabris* (BS = 29). We found that the *T. atlantica* ancestor diverged from the
350 remaining *Trachylepis* in the Miocene, approximately 17 Ma (between 10 and 27 Ma) in tropical
351 Africa. The younger diversification of *T. atlantica* indicates that the crossing of this species to
352 Fernando de Noronha occurred more recently than did the occupation of South America by the
353 CAM clade. Our analyses also suggested that once the ancestors of this major *Trachylepis* clade
354 reached Africa, dispersal events from the African continent occurred to Madagascar and nearby
355 islands at least three times, in addition to the dispersal to the Neotropics (*T. atlantica*). Our
356 results showed that a monophyletic Madagascan *Trachylepis* (BS = 94) diverged from its sister
357 group approximately 19 Ma (12 – 32 Ma) (BS = 23).

358 The ANOVA was used to test whether the full four-parameter GeoSSE model of the *NW*/
359 \overline{NW} comparison (model 1) was statistically favored over simpler alternative models (models 2-
360 4). When we constrained speciation rates to be equal (model 2) and to present equal speciation
361 and extinction rates (model 4), the full model was supported over these alternative models ($p =$
362 0.00782 and $p = 0.02900$, respectively). The comparison with the model that constrained
363 extinction rates (model=3), however, was not significantly different ($p = 0.15575$).

364 GeoSSE analysis of the difference between the posterior distributions of speciation rates
365 in *NW*/ \overline{NW} lineages indicated a positive credible interval (CI) (0.005 – 0.113), suggesting that
366 the speciation rates of South American clades (*NW*) were indeed higher than those of the
367 remaining lineages (\overline{NW}). In BAMM, however, we failed to find a significant difference
368 between the posterior distributions of speciation rates (CI: -0.030 – 0.031). We also found no

369 evidence for diversification shifts during mabuyine diversification. However, the
370 macroevolutionary cohort matrix suggested heterogeneous macroevolutionary rate regimes in the
371 South American Mabuyinae and the remaining clades (Figure 2a). In both GeoSSE and BAMM
372 analyses, we failed to find differences between the extinction rates (CI_{GeoSSE} : -0.036 – 0.074,
373 CI_{BAMM} : -0.027 – 0.027) and between the net diversification rates (CI_{GeoSSE} : -0.010 – 0.090,
374 CI_{BAMM} : -0.027 – 0.027) (Figure 2b).

375 Concerning the influence of viviparity on diversification rates, no submodels were
376 supported over the unconstrained model ($p > 0.05$). STRAPP analysis failed to find any
377 correlation between diversification rates and mode of reproduction ($p > 0.05$). We also found no
378 differences between the means obtained from the MCMC of the BiSSE (CI: -0.018 – 0.125, -
379 0.038 – 0.055, -0.051 – 0.049, respectively for speciation, extinction, and transition rates).

380 The ancestor of CAM and their *Trachylepis* sister clade was recovered as viviparous by
381 BayesTraits ($P_{\text{BTML}}=0.751$; $P_{\text{BTBA}}=0.787$) and as oviparous by BiSSE ($P_{\text{BiSSE}}=1$), while the
382 ancestor of CAM alone was recovered as viviparous by all approaches ($P_{\text{BiSSE}}=0.953$;
383 $P_{\text{BTML}}=0.992$; $P_{\text{BTBA}}=0.983$), suggesting that the ancestral species that colonised South America
384 was likely viviparous (Figure 2a). The ancestor of the subfamily Mabuyinae was inferred as
385 oviparous ($P_{\text{BiSSE}}=1$; $P_{\text{BTML}}=0.983$; $P_{\text{BTBA}}=0.980$). Viviparity seems to have emerged several
386 times in the genus *Trachylepis*, as well as in the ancestor of *Chioninia* ($P_{\text{BiSSE}}=0.952$;
387 $P_{\text{BTML}}=0.984$; $P_{\text{BTBA}}=0.971$).

388 According to PIC results, SVL measurement and body mass were correlated ($p_{\text{LRP}} <$
389 0.01), however, we had found differences in their evolutionary rates. The mean rates of trait
390 evolution of SVL and body mass were smaller in the New World clade than in the \overline{NW} lineages.
391 However, these differences were not significant. In BAMM, we found an increase in the rate of

392 SVL trait evolution in genus *Chioninia*. Only one clade presented an increase in the rate of body
393 mass trait evolution: the Seychelles *Trachylepis* (*T. wrightii* and *T. brevicollis*). STRAPP
394 analysis failed to find a significant correlation between the rate of species diversification and the
395 rate of SVL or body mass trait evolution ($p > 0.05$).

396 **Discussion**

397

398 Our analyses based on a fossil-calibrated timetree support the hypothesis that the
399 occupation of South America by the ancestors of the Continental America Mabyuinae (CAM)
400 clade occurred between the Eocene and the Oligocene from the Saharo-Arabian region,
401 corroborating recent estimates (e.g. Pinto-Sánchez *et al.* 2015; Karin *et al.*, 2016). This
402 colonization occurred independently of that of *Trachylepis atlantica*, which split from its tropical
403 African sister clade between the Oligocene and the Miocene. Therefore, our results corroborate
404 the hypothesis that the ancestor of *T. atlantica* dispersed from tropical Africa as suggested by
405 Mausfeld *et al.* (2002). The divergence between *T. atlantica* and its African ancestors was older
406 than the estimated age of the formation of the Fernando de Noronha archipelago (12.3–1.7 Ma;
407 Almeida, 2002). Thus, it is unlikely that the ancestors of *T. atlantica* reached South America in a
408 single transoceanic dispersal event. It is more probable to hypothesize a complex dispersal
409 scenario, with a series of dispersals through a transatlantic island corridor leading to Fernando de
410 Noronha, consistent with the Atlantogea model (Oliveira *et al.* 2009; Ezcurra and Agnolin,
411 2012). This stepping-stone mode of dispersal could explain the discrepancy between the ages of
412 genetic divergence and the formation of the archipelago because it would dissociate the
413 geological formation of the Fernando de Noronha archipelago from the genetic isolation of the
414 ancestor of *T. atlantica*. This result must be interpreted cautiously because choosing between
415 alternative biogeographical scenarios is influenced by the inferred timescale. The lack of extant
416 and extinct mabyuine species may have impacted divergence time estimates.

417 The age of the crown node of living CAM species was inferred to be much older than the
418 estimates reported by Carranza and Arnold (2003), 7–9 Ma. The credibility interval of our

419 estimate (12–31 Ma), however, contains the ages inferred by Miralles and Carranza (2010),
420 Hedges and Conn (2012) and Karin *et al.* (2016), which dated this node at approximately 14 Ma.
421 Our results were still inconclusive to establish the precise sequence of events that gave rise to the
422 current geographical distribution of both CAM and *T. atlantica*. Nevertheless, the evolution of
423 these two American lineages of Mabuyinae corroborates a faunal connection between Africa and
424 the Neotropics, and suggests that dispersals may have occurred through island hopping, which is
425 more likely than a single sweepstake event across the Atlantic Ocean. In this sense, it is
426 interesting to mention that a species has been described in the mid-Atlantic Ascension Island by
427 Gray in 1838, which was subsequently assigned to genus *Mabuya*; however, no recent systematic
428 re-evaluation of this specimen is available (Mausfeld and Vrcibradic, 2002).

429 The arrival of Mabuyinae to South America seems to have changed the diversification
430 rate regime of this lineage. The evolutionary rates of both body mass and SVL traits were not
431 significantly altered after the arrival of the ancestors of New World clades, but the increases in
432 rates of both traits were found in island groups, such in Cape Verde's *Chioninia* and Seychelles'
433 *Trachylepis*. The viviparous CAM clade presents peculiar reproductive traits, such as a
434 specialized chorioallantoic placenta that provides fetal nutrition, similarly to eutherian mammals
435 (Vrcibradic and Rocha, 2011). This character was suggested to be synapomorphous by Mausfeld
436 *et al.* (2002). According to our analysis, the CAM ancestor was already viviparous, in agreement
437 with the large-scale analysis of Squamates (Pyron and Burbrink, 2013). However, Pyron and
438 Burbrink (2013) suggested an early origin of viviparity in Mabuyinae and multiple transitions to
439 oviparity, including the clade consisting of *Chioninia* and CAM + *Heremites*. On the other hand,
440 possibly because of topological differences, we estimated that the ancestor of Mabuyinae was
441 oviparous and multiple reversions to viviparity occurred later along the evolution of the lineage.

442 Regarding the biogeographic history of the subfamily Mabuyinae, Greer (1970), based on
443 the primitive characteristics of Asian Mabuyinae, suggested that the ancestors of this subfamily
444 first dispersed from Asia. Other works reasserted this hypothesis, although no formal statistical
445 analyses were conducted (Honda *et al.*, 1999; 2003; Karin *et al.*, 2016). Our results suggest that
446 the early members of Mabuyinae dispersed to Africa and then reached South America and
447 several oceanic islands. The inferred time-dated phylogeny and biogeographic reconstruction
448 similarly suggest an Oriental ancestral distribution, as corroborated by the distribution of the
449 genera *Lankascincus* and *Ristella*, which were recovered as sister clades of Mabuyinae and are
450 geographically distributed in the Oriental region (Sri Lanka and the Indian, respectively). Karin
451 *et al.*, 2016 inferred that *Eutropis*, instead of *Dasia*, was the first Mabuyinae offshoot.
452 Nevertheless, as both genera are distributed in the Oriental region, this topological rearrangement
453 would not significantly alter the ancestral area reconstruction.

454 Finally, this study provides an updated timescale and estimates of macroevolutionary
455 regimes of the diversification of the subfamily Mabuyinae. Our focus was the occupation of the
456 South American continent by the subfamily Mabuyinae through an Oligocene/Eocene
457 transoceanic connection (Atlantogea), which could be responsible for approximately 29% of the
458 South American mammal diversity, suggesting the importance of this event to the extant
459 vertebrate diversity in South America (Marshall *et al.*, 1982). CAM and *T. atlantica* are the only
460 representatives of the family Scincidae in South America accounting for 4% of the
461 approximately 1,560 squamate species on this continent (Uetz, 2000). Although there are species
462 of other subfamilies of Scincidae in Central America, these species seem to have never crossed
463 the Isthmus of Panama. The converse also seems correct because the only mabuyine genus
464 (*Marisora*) that partially occupied Central America based on our results had arrived via an

465 intermediate dispersion through the West Indies. If this is the case, no representative of Scincidae
466 would be found in present day South American fauna in the absence of this Atlantogea
467 connection. Our results give an overall picture of the timing, biogeography and
468 macroevolutionary dynamics associated with the arrivals of the ancestors of this exceptional case
469 of transoceanic dispersal in two closely related lineages.

470

471 **Acknowledgements**

472

473 This study is part of the Doctoral Thesis of AGP from the Genetics Graduation Program
474 at the Federal University of Rio de Janeiro.

475 **References**

476

477 Aberer AJ, Krompass D, Stamatakis A. 2013. Pruning Rogue Taxa Improves Phylogenetic

478 Accuracy: An Efficient Algorithm and Webservice. *Systematic Biology* 62:162–166.

479 Albert EM, San Mauro D, García-París M, Rüber L, Zardoya R. 2009. Effect of taxon sampling

480 on recovering the phylogeny of squamate reptiles based on complete mitochondrial genome

481 and nuclear gene sequence data. *Gene* 441:12–21.482 Almeida FFM. 2002. Arquipélago de Fernando de Noronha. *Sítios geológicos e paleontológicos*483 *do Brasil* 66:361–368.

484 Barker FK, Burns KJ, Klicka J, Lanyon SM, Lovette IJ. 2015. New insights into New World

485 biogeography, An integrated view from the phylogeny of blackbirds, cardinals, sparrows,

486 tanagers, warblers, and allies. *The Auk* 132:333–348.

487 Benton MJ, Donoghue P, Asher RJ. 2015. Constraints on the timescale of animal evolutionary

488 history. *Palaeontologia Electronica* 18.1.1FC:1–106.

489 Böhme M. 2010. Ectothermic vertebrates (Actinopterygii, Allocaudata, Urodela, Anura,

490 Crocodylia, Squamata) from the Miocene of Sandelzhausen (Germany, Bavaria). and their

491 implications for environment reconstruction and palaeoclimate. *Paläontologische Zeitschrift*

492 84:3–41.

493 Böttcher R., Heizmann EPJ, Rasser MW, Ziegler R. 2009. Biostratigraphy and palaeoecology of

494 a Middle Miocene (Karpathian, MN 5) fauna from the northern margin of the North Alpine

495 Foreland Basin (Oggenhausen 2, SW' Germany). *Neues Jahrbuch für Geologie und*496 *Paläontologie - Abhandlungen* 254:237–260.497 Briggs JC. 2003. Fishes and Birds, Gondwana Life Rafts Reconsidered. *Systematic Biology*

- 498 52:548–553.
- 499 Carranza S, Arnold EN. 2003. Investigating the origin of transoceanic distributions, mtDNA
500 shows *Mabuia* lizards (Reptilia, Scincidae) crossed the Atlantic twice. *Systematics and*
501 *Biodiversity* 1:275–282.
- 502 Castresana J. 2000. Selection of Conserved Blocks from Multiple Alignments for Their Use in
503 Phylogenetic Analysis. *Molecular Biology and Evolution* 17:540–552.
- 504 Das I. 2010. *A Field Guide To The Reptiles Of South-East Asia*, London: New Holland
505 Publishers.
- 506 de Oliveira FB, Molina EC, Marroig G. 2009. Paleogeography of the South Atlantic, a Route for
507 Primates and Rodents into the New World? In Garber PA, Estrada A, Bicca-Marques JC,
508 Heymann EW, Strier KB, ed. *South American Primates, Developments in Primatology:*
509 *Progress and Prospects*. New York: Springer. p 55–68.
- 510 de Queiroz A. 2005. The resurrection of oceanic dispersal in historical biogeography. *Trends in*
511 *Ecology and Evolution* 20:68–73.
- 512 de Queiroz A. 2014. *The Monkey's Voyage, How Improbable Journeys Shaped the History of*
513 *Life*. New York: Basic Books.
- 514 Edgar RC. 2004. MUSCLE, multiple sequence alignment with high accuracy and high
515 throughput. *Nucleic Acids Research* 32:1792–1797.
- 516 Estes R. 1983. *Encyclopedia of Paleoherpetology*. Stuttgart: Gustav Fischer Verlag.
- 517 Ezcurra MD, Agnolin FL. 2012. A New Global Palaeobiogeographical Model for the Late
518 Mesozoic and Early Tertiary. *Systematic Biology* 61:553–566.
- 519 FitzJohn RG. 2012. Diversitree, comparative phylogenetic analyses of diversification in R.
520 *Methods in Ecology and Evolution* 3:1084–1092.

- 521 Goldberg EE, Lancaster LT, Ree RH. 2011. Phylogenetic Inference of Reciprocal Effects
522 between Geographic Range Evolution and Diversification. *Systematic Biology* 60:451–465.
- 523 Gouy M, Guindon S, Gascuel O. 2010. SeaView Version 4, A Multiplatform Graphical User
524 Interface for Sequence Alignment and Phylogenetic Tree Building. *Molecular Biology and*
525 *Evolution* 27:221–224.
- 526 Greer AE. 1970. A subfamilial classification of scincid lizards. *Bull. Mus. comp. Zool. Harvard*
527 139:151–183.
- 528 Heads M. 2011. Old Taxa on Young Islands, A Critique of the Use of Island Age to Date Island-
529 Endemic Clades and Calibrate Phylogenies. *Systematic Biology* 60:204–218.
- 530 Hedges SB, Conn CE. 2012. A new skink fauna from Caribbean islands (Squamata, Mabuyidae,
531 Mabuyinae). *Zootaxa* 3288:1–244.
- 532 Heibl C. 2015. Phyloch. Available at <http://www.christophheibl.de/Rpackages.html>.
- 533 Holman JA. 1966. A small Miocene herpetofauna from Texas. *Quarterly Journal of the Florida*
534 *Academy of Sciences* 29:267–275.
- 535 Holman JA. 1981. A herpetofauna from an early extension of the Harrison Formation (early
536 Miocene, Arikareean), Cherry County, Nebraska. *Journal of Vertebrate Paleontology* 1:49–
537 56.
- 538 Honda M, Ota H, Kobayashi M, Nabhitabhata J, Yong H, and Hikida T. 1999. Evolution of
539 Asian and African Lygosomine Skinks of the *Mabuya* Group (Reptilia, Scincidae), A
540 Molecular Perspective. *Zoological Science* 16:979–984.
- 541 Honda M, Ota H, Kohler G, Ineich I, Chirio L, Chen S-L, Hikida T. 2003. Phylogeny of the
542 Lizard Subfamily Lygosominae (Reptilia, Scincidae), with Special Reference to the Origin
543 of the New World Taxa. *Genes Genet. Syst.* 78:17–80.

- 544 Joeckel RM. 1988. A new late Miocene herpetofauna from Franklin County, Nebraska. *Copeia*
545 3:787–789.
- 546 Karin BR, Metallinou M, Weinell JL, Jackman TR, Bauer AM. 2016. Resolving the higher-order
547 phylogenetic relationships of the circumtropical Mabuya group (Squamata: Scincidae): An
548 out-of-Asia diversification. *Molecular Phylogenetics and Evolution* 102:220–232.
- 549 Katoh K, Standley DM. 2013. MAFFT Multiple Sequence Alignment Software Version 7,
550 Improvements in Performance and Usability. *Molecular Biology and Evolution* 30:772–780.
- 551 Lanfear R, Calcott B, Ho SYW, Guindon S. 2012. PartitionFinder, Combined Selection of
552 Partitioning Schemes and Substitution Models for Phylogenetic Analyses. *Molecular*
553 *Biology and Evolution* 29:1695–1701.
- 554 Le M, Raxworthy CJ, Mccord WP, Mertz L. 2006. A molecular phylogeny of tortoises
555 (Testudines, Testudinidae). based on mitochondrial and nuclear genes. *Molecular*
556 *Phylogenetics and Molecular Phylogenetics and Evolution* 40:517–531.
- 557 Leigh EG, O'Dea A, Vermeij GJ. 2013. Historical biogeography of the Isthmus of Panama.
558 *Biological Reviews* 89:148–172.
- 559 Leite RN, Kolokotronis S-O, Almeida FC, Werneck FP, Rogers DS, Weksler M. 2014. In the
560 Wake of Invasion, Tracing the Historical Biogeography of the South American Cricetid
561 Radiation (Rodentia, Sigmodontinae). *PLoS ONE* 9:e100687.
- 562 Lima A, Harris DJ, Rocha S, Miralles A, Glaw F, Vences M. 2013. Phylogenetic relationships of
563 *Trachylepis* skink species from Madagascar and the Seychelles (Squamata, Scincidae).
564 *Molecular Phylogenetics and Evolution* 67:615–620.
- 565 Linder HP, Hardy CR, Rutschmann F. 2005. Taxon sampling effects in molecular clock dating,
566 An example from the African Restionaceae. *Molecular Phylogenetics and Evolution* 35:569–

- 567 582.
- 568 Lomolino MV. 2010. *Biogeography*. Sunderland: Sinauer Associates.
- 569 Loss-Oliveira L, Aguiar B, Schrago CG. 2012. Testing Synchrony in Historical Biogeography:
570 The Case of New World Primates and Hystricognathi Rodents. *Evolutionary Bioinformatics*
571 8:127–137.
- 572 Marshall LG, Webb SD, Sepkoski Jr JJ, Raup DM. 1982. Mammalian evolution and the Great
573 American Interchange. *Science* 215:1351–1357.
- 574 Matzke NJ. 2013. Probabilistic historical biogeography, new models for founder-event
575 speciation, imperfect, d. etection., and fossils allow improved accuracy and model-testing.
576 *Frontiers of Biogeography* 5:242–248.
- 577 Matzke NJ. 2014. Model Selection in Historical Biogeography Reveals that Founder-Event
578 Speciation Is a Crucial Process in Island Clades. *Systematic Biology* 63: 951–970.
- 579 Mausfeld P. 2000. First Data on the Molecular Phylogeography of Scincid Lizards of the Genus
580 *Mabuya*. *Molecular Phylogenetics and Evolution* 17:11–14.
- 581 Mausfeld P, Vrcibradic D. 2002. On the Nomenclature of the Skink (*Mabuya*). Endemic to the
582 Western Atlantic Archipelago of Fernando de Noronha, Brazil. *Journal of Herpetology*
583 36:292–295.
- 584 Mausfeld P, Schmitz A, Bohme W, Misof B, Vrcibradic D, Rocha CFD. 2002. Phylogenetic
585 Affinities of *Mabuya atlantica* Schmidt, 1945, Endemic to the Atlantic Ocean Archipelago
586 of Fernando de Noronha (Brazil), Necessity of Partitioning the Genus *Mabuya* Fitzinger,
587 1826 (Scincidae, Lygosominae). *Zoologischer Anzeiger* 241:281–293.
- 588 Meiri S. 2010. Length-weight allometries in lizards. *Journal of Zoology* 281:218–226.
- 589 Meiri S, Bauer AM, Chirio L, Colli GR, Das I, Doan TM, Feldman A, Herrera F-C, Novosolov

- 590 M, Pafilis P, Pincheira-Donoso D, Powney G, Torres-Carvajal O, Uetz P, Van Damme R.
591 2013. Are lizards feeling the heat? A tale of ecology and evolution under two temperatures.
592 *Global Ecology and Biogeography* 22: 834–845.
- 593 Mello B, Schrago CG. 2012. Incorrect handling of calibration information in divergence time
594 inference, an example from volcanic islands. *Ecology and Evolution* 2:493–500.
- 595 Miralles A, Carranza S. 2010. Systematics and biogeography of the Neotropical genus *Mabuya*,
596 with special emphasis on the Amazonian skink *Mabuya nigropunctata* (Reptilia, Scincidae).
597 *Molecular Phylogenetics and Evolution* 54:857–869.
- 598 Morrone JJ. 2014. Biogeographical regionalisation of the Neotropical region. *Zootaxa* 3782:1–
599 110.
- 600 Mulcahy DG, Noonan BP, Moss M, Townsend TM, Reeder TW, Sites Jr JW, Wiens JJ. 2012.
601 Estimating divergence dates and evaluating dating methods using phylogenomic and
602 mitochondrial data in squamate reptiles. *Molecular Phylogenetics and Evolution* 65:974–
603 991.
- 604 Pagel M, Meade A, Barker D. 2004. Bayesian Estimation of Ancestral Character States on
605 Phylogenies. *Systematic Biology* 53:673–684.
- 606 Pinto-Sanchez NR, Calderón-Espinosa ML, Miralles A, Crawford AJ, Ramírez-Pinilla MP.
607 2015. Molecular phylogenetics and biogeography of the Neotropical skink genus *Mabuya*
608 Fitzinger (Squamata: Scincidae) with emphasis on Colombian populations. *Molecular*
609 *Phylogenetics and Evolution* 93:188–211.
- 610 Poux C, Chevret P, Huchon D, de Jong WW, Douzery EJP. 2006. Arrival and Diversification of
611 Caviomorph Rodents and Platyrrhine Primates in South America. *Systematic Biology*
612 55:228–244.

- 613 Pyron RA. 2014. Biogeographic Analysis Reveals Ancient Continental Vicariance and Recent
614 Oceanic Dispersal in Amphibians. *Systematic Biology* 63:779–797.
- 615 Pyron RA, Burbrink FT. 2013. Early origin of viviparity and multiple reversions to oviparity in
616 squamate reptiles. *Ecology Letters* 17:13–21.
- 617 Pyron R, Burbrink FT, Wiens JJ. 2013. A phylogeny and revised classification of Squamata,
618 including 4161 species of lizards and snakes. *BMC Evolutionary Biology* 13:93.
- 619 Rabosky DL. 2014. Automatic detection of key innovations, rate, shifts, and diversity-
620 dependence on phylogenetic trees. *PLoS ONE* 9:e89543.
- 621 Rabosky DL, Grundler M, Anderson C, Title CP, Shi JJ, Brown JW, Huang H, Larson JG. 2014.
622 BAMMtools, an R package for the analysis of evolutionary dynamics on phylogenetic trees.
623 *Methods in Ecology and Evolution* 5:701–707.
- 624 Renner SS. 2004. Plant dispersal across the tropical atlantic by wind and sea currents.
625 *International Journal of Plant Science* 165:S23–S33.
- 626 Rowe TB, Cifelli RL, Lehman TM, Weil A. 1992. The Campanian Terlingua local fauna, with a
627 summary of other vertebrates from the Aguja Formation. *Journal of Vertebrate Paleontology*
628 12:472–493.
- 629 Sanmartín I, van der Mark P, Ronquist F. 2008. Inferring dispersal, a Bayesian approach to
630 phylogeny-based island biogeography, with special reference to the Canary Islands. *Journal*
631 *of Biogeography* 35:428–449.
- 632 Schrago CG, Mello B, Soares AER. 2013. Combining fossil and molecular data to date the
633 diversification of New World Primates. *Journal of Evolutionary Biology* 26: 2438–2446.
- 634 Schrago CG, Menezes AN, Moreira MAM, Pissinatti A, Seuánez HN. 2012. Chronology of
635 Deep Nodes in the Neotropical Primate Phylogeny, Insights from Mitochondrial Genomes.

- 636 *PLoS ONE* 7: e51699.
- 637 Simpson GG. 1950. History of the Fauna of Latin America. *American Scientist* 38: 361–389.
- 638 Simpson GG. 1953. The Major Features of Evolution. Columbia University Press, New York.
- 639 Sindaco R, Metallinou M, Pupin F, Fasola M, Carranza S. 2012. Forgotten in the ocean,
640 systematics, biogeography and evolution of the *Trachylepis* skinks of the Socotra
641 Archipelago. *Zoologica Scripta* 41:346–362.
- 642 Soares A, Schrago CG. 2012. The Influence of Taxon Sampling and Tree Shape on Molecular
643 Dating, An Empirical Example from Mammalian Mitochondrial Genomes. *Bioinformatics
644 and Biology Insights* 6:129–143.
- 645 Stamatakis A. 2014. RAxML Version 8, A tool for Phylogenetic Analysis and Post-Analysis of
646 Large Phylogenies. *Bioinformatics* 30:1312–1313.
- 647 Stamatakis A, Hoover P, Rougemont J. 2008. A Rapid Bootstrap Algorithm for the RAxML
648 Web Servers. *Systematic Biology* 57:758–771.
- 649 Talavera G, Castresana J. 2007. Improvement of Phylogenies after Removing Divergent and
650 Ambiguously Aligned Blocks from Protein Sequence Alignments. *Systematic Biology*
651 56:564–577.
- 652 Teeling EC. 2005. A Molecular Phylogeny for Bats Illuminates Biogeography and the Fossil
653 Record. *Science* 307:580–584.
- 654 Uetz P. 2000. How many Reptile Species? *Herpetological Review* 31: 13–15.
- 655 Uetz, P. 1996. The Reptile Database. Available at <http://www.reptile-database.org> (accessed 15
656 January 2017).
- 657 Venczel M, Hír J. 2013. Micro-computed tomography study of a three-dimensionally preserved
658 neurocranium of *Albanerpeton* (Lissamphibia, Albanerpetontidae) from the Pliocene of

- 659 Hungary. *Journal of Vertebrate Paleontology* 33:568–587.
- 660 Vidal N, Azvolinsky A, Cruaud C, Hedges SB. 2008. Origin of tropical American burrowing
661 reptiles by transatlantic rafting. *Biology Letters* 4:115–118.
- 662 Vitt LJ., Caldwell MW. 2009. *Herpetology: An Introductory Biology of Amphibians and*
663 *Reptiles*. Burlington: Elsevier.
- 664 Voloch CM, Vilela JF, Loss-Oliveira L, Schrago CG. 2013. Phylogeny and chronology of the
665 major lineages of New World hystricognath rodents, insights on the biogeography of the
666 Eocene/Oligocene arrival of mammals in South America. *BMC Research Notes* 6:1–9.
- 667 Voorhies MR, Holman JA, Xiang-xu X. 1987. The Hottell Ranch rhino quarries (basal Ogallala;
668 medial Barstovian), Banner County, Nebraska; Part I; Geologic setting, faunal lists, lower
669 vertebrates. *Contributions to Geology, University of Wyoming* 25:55–69.
- 670 Vrcibradic D, Rocha CFD. 2011. An overview of female reproductive traits in South American
671 *Mabuya* (Squamata, Scincidae), with emphasis on brood size and its correlates. *Journal of*
672 *Natural History* 45:813–825.
- 673 Whiting AS, Sites Jr JW, Pellegrino KCM, Rodrigues MT. 2006. Comparing alignment methods
674 for inferring the history of the new world lizard genus *Mabuya* (Squamata, Scincidae).
675 *Molecular Phylogenetics and Evolution* 38:719–730.
- 676 Yang Z. 2007. PAML 4: Phylogenetic Analysis by Maximum Likelihood. *Molecular Biology*
677 *and Evolution* 24:1586–1591.

Table 1 (on next page)

General information on the loci used in this study.

1

	<i>12S</i>	<i>16S</i>	<i>enol</i>	<i>cytb</i>	<i>cmos</i>	<i>gapdh</i>	<i>myh</i>	<i>gpr149</i>	Total
Number of sequenced species	214	194	70	153	146	47	51	73	218
Alignment length	366	464	192	1,033	894	380	133	669	4,131
Frequency of sites with missing data	0.12	0.20	0.74	0.38	0.40	0.81	0.81	0.72	0.47
Frequency of indels	0.02	0.03	0.01	0.16	0.22	0.04	0.01	0.01	0.10

2

Table 2 (on next page)

Model comparisons performed in 'diversitree'.

Constraints in the macroevolutionary models subjected to ANOVA for differences in the rates of speciation (λ) and extinction (μ) between New World (NW) and Old World (NW) areas (GeoSSE) and between viviparous (V) and non-viviparous (V) lineages (BiSSE).

Model	Approach	Constrains	Parameters
Reduced full	GeoSSE	NA	$\lambda_{NW}, \lambda_{\overline{NW}}, \mu_{NW}, \mu_{\overline{NW}}$
	BiSSE	NA	$\lambda_V, \lambda_{\overline{V}}, \mu_V, \mu_{\overline{V}}$
Equal speciation	GeoSSE	$\lambda_{NW} = \lambda_{\overline{NW}}$	$\lambda, \mu_{NW}, \mu_{\overline{NW}}$
	BiSSE	$\lambda_V = \lambda_{\overline{V}}$	$\lambda, \mu_V, \mu_{\overline{V}}$
Equal extinction	GeoSSE	$\mu_{NW} = \mu_{\overline{NW}}$	$\lambda_{NW}, \lambda_{\overline{NW}}, \mu$
	BiSSE	$\mu_V = \mu_{\overline{V}}$	$\lambda_V, \lambda_{\overline{V}}, \mu$
Equal diversification	GeoSSE	$\lambda_{NW} = \lambda_{\overline{NW}}$	λ, μ
		$\mu_{NW} = \mu_{\overline{NW}}$	
	BiSSE	$\lambda_V = \lambda_{\overline{V}}$	λ, μ
		$\mu_V = \mu_{\overline{V}}$	

1
2
3

Table 3 (on next page)

Model comparisons performed in BioGeoBEARS

Likelihood-ratio tests between null models (DIVALIKE and DEC) and more sophisticated models with the addition of the founder-event speciation (+J) (DIVALIKE+J and DEC+J). (LnL) Likelihood value. (DF) Degrees of freedom for the chi-square test.

model	Null model	LnLalt	LnLnull	DF	pval
DEC+J	DEC	-94.34	-112.8	1	1.20E-09
DIVALIKE+J	DIVALIKE	-95.65	-119.2	1	6.70E-12

1

Figure 1

Time-dated phylogeny of the Mabuyinae with ancestral area reconstruction

Maps depict putative dispersals and vicariant events that culminated in the occupation of South America by this group. Ancestral area reconstruction was based on the results from DEC+J because this model produced a significantly higher log-likelihood score. The black regions in pie charts represent bootstrap supports.

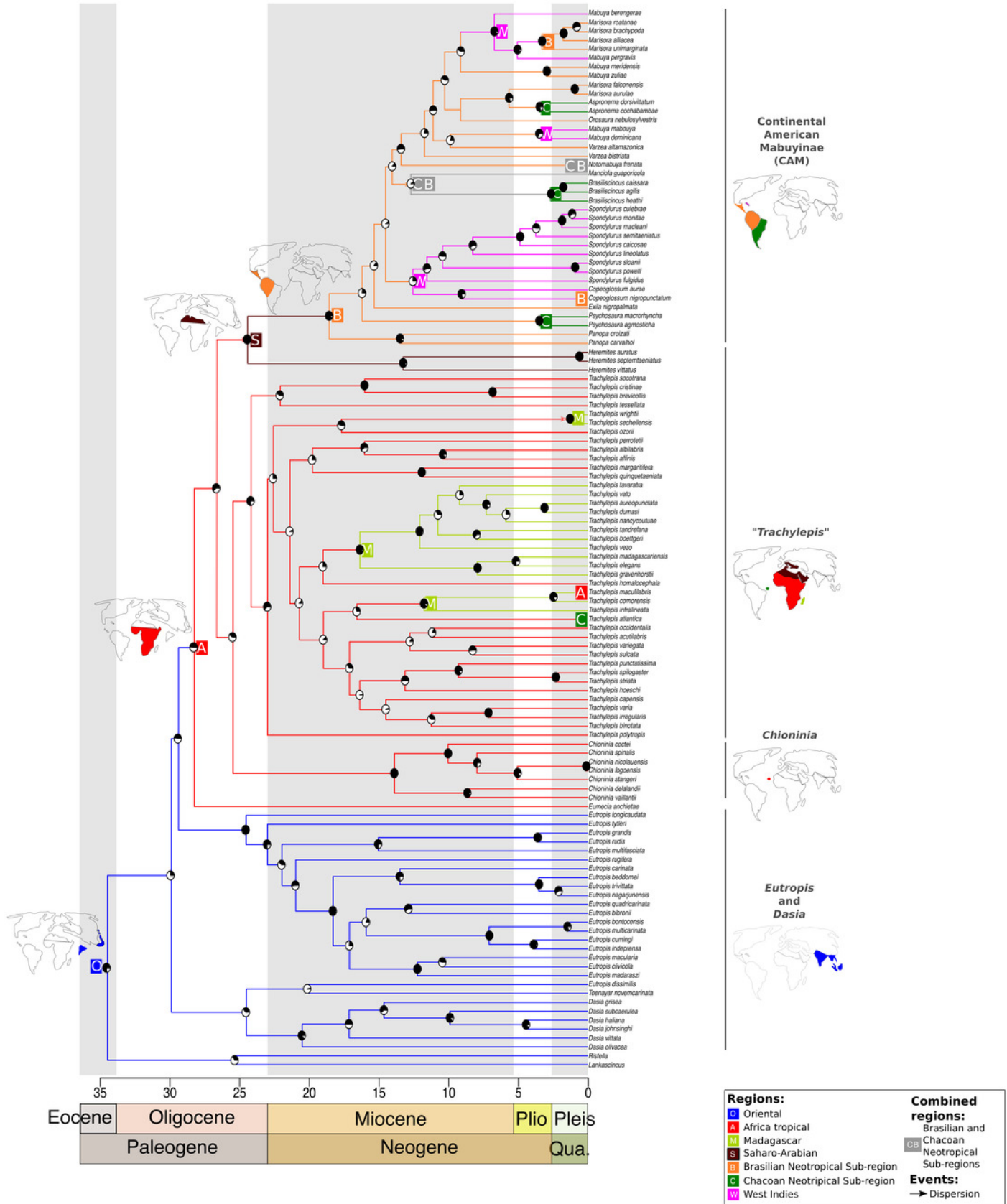


Figure 2

Macroevolutionary cohort matrix for the Mabuyinae subfamily.

A. Illustration of the macroevolutionary rates for the mabuyine lineage obtained using BAMB. For reference, the BAMB tree was plotted at the upper margin of the figure. The pairwise probability that any two species share a common macroevolutionary rate dynamic was indicated by the color of each individual cell. Color scale is indicated at the right. The coral and brown circles in the upper tree represent the shifts found with BAMB in the traits SVL and body mass, respectively. In the left most tree topology, pie charts at nodes indicate the mode of reproduction inferred by BayesTraits, according to the probability of occurrence of each character. Red represents viviparity, and black represents oviparity. B. Marginal distributions of macroevolutionary rates inferred in BAMB and GeoSSE were also depicted for New World (green) and non-New World samples (orange).

